

**Designing a Polycationic Probe for Simultaneous Enrichment and Detection of  
MicroRNAs in a Nanopore**

Kai Tian, Zhaojian He, Yong Wang, Shi-Jie Chen, Li-Qun Gu

**Supplementary Materials**

**Table S1.** Sequences of miRNAs and probe used in this study

Target and probe	Sequence
P <sub>7b</sub>	N' - YGRKKRRQRRR - AACCA <u>C</u> ACAAA - C'
Let-7b	5' - ugagguaguagguugugugguu - 3'
Let-7c	5' - ugagguaguagguuguaugguu - 3'
miR-155	5' - uuaaugcuaaucgugauaggggu - 3'
miR-21	5' - uagcuuaucaagacugauguuga - 3'

**Table S2.** Properties of the Let-7b•P<sub>7b</sub> signatures in the absence and in the presence of background RNAs miR-155 and miR-21

Properties	Without background	With background	<i>t</i> -test ( <i>p</i> )
$I_R$ (pA)	74.0±1.5	73.2±1.4	0.51
$\tau_{off}$ (ms)	28±4	24±5	0.58
$f$ (s <sup>-1</sup> )	8.0±0.9	7.1±3.7	0.42

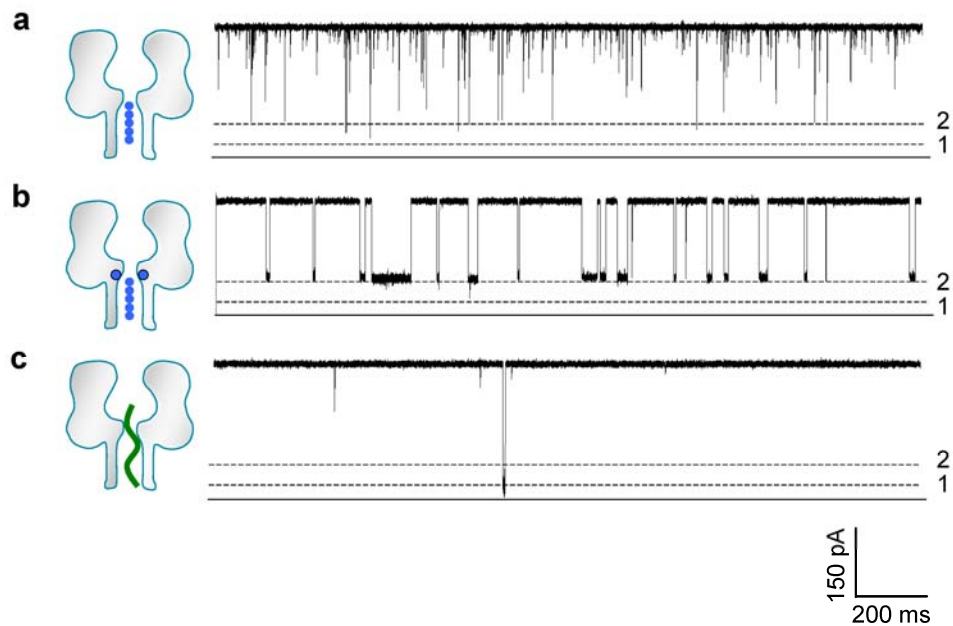


**Figure S1.** Current traces showing translocation or binding of various polymers in the nanopores. The currents were recorded at +180 mV in 1 M KCl solution buffered with 10 mM Tris (pH7.2). All polymers were added in trans solution. **a**, Translocation of the HIV-TAT peptide in the K131D pore; **b**, Encapsulation of the HIV-TAT peptide in the M13R pore. Blue dots marked in the nanopore model represents the arginine ring (R113) constructed in the constrictive region lining the pore lumen; and **c**, Translocation of PNA alone in the K131D pore. PNA rarely translocate or binds the pore from trans opening.

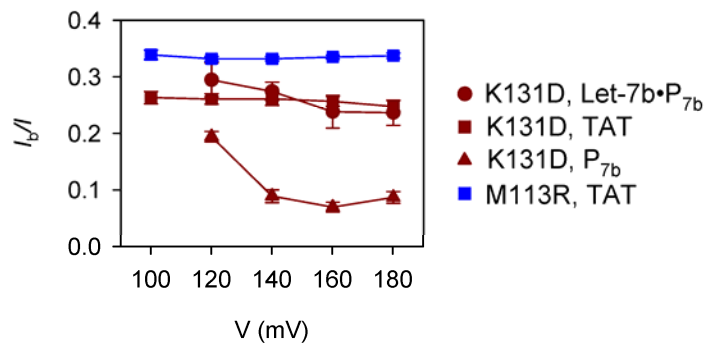


**Figure S2.** Voltage-dependent relative block currents for various polymers in the nanopores. The currents were recorded at +180 mV in 1 M KCl solution buffered with 10 mM Tris (pH7.2). All polymers were added in trans solution. Red circle: Let-7b•P<sub>7b</sub> complex in the K131D pore; Red square: TAT peptide in the K131D pore; Red triangle, P<sub>7b</sub> probe in the M113R pore; and blue square: TAT peptide in the M113R pore.

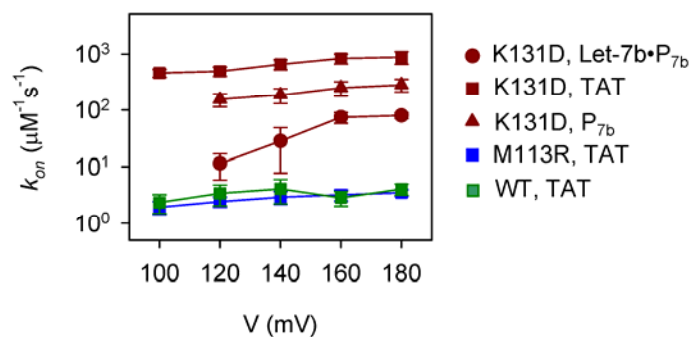


**Figure S3.** Voltage-dependent capture rates for trapping various polymers in the nanopores. The currents were recorded at +180 mV in 1 M KCl solution buffered with 10 mM Tris (pH7.2). All polymers were added in trans solution. Red circle: Let-7b•P<sub>7b</sub> complex in the K131D pore; Red square: TAT peptide in the K131D pore; Red triangle, P<sub>7b</sub> probe in the M113R pore; and blue square: TAT peptide in the M113R pore.

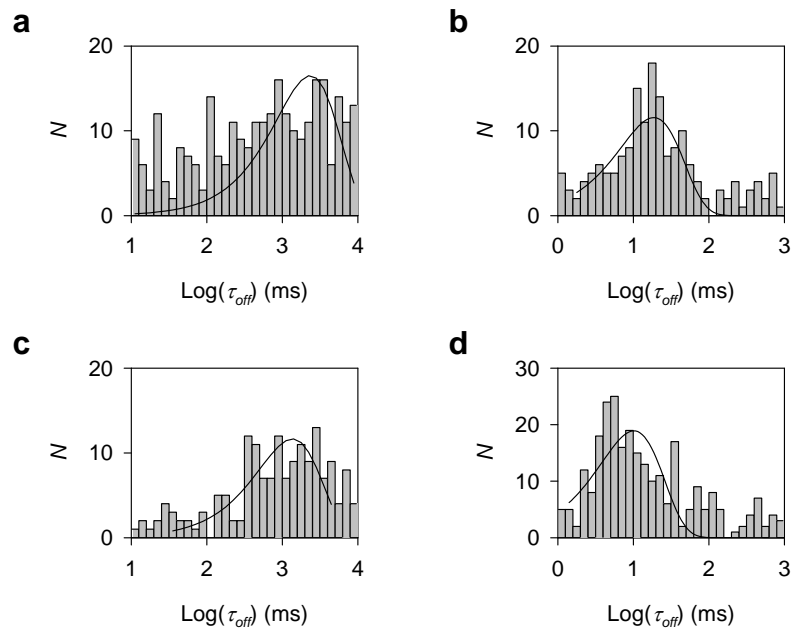


**Figure S4.** Duration histograms of signature blocks for fully-matched Let-7b•P<sub>7b</sub> and one-mismatched Let-7c•P<sub>7b</sub> at different voltages. **a** and **b.** were for (a) Let-7b•P<sub>7b</sub>,  $\tau_{off}=2.3\pm0.5$  s, and (b) Let-7c•P<sub>7b</sub>,  $\tau_{off}=19\pm0.7$  ms at +140 mV; **c** and **d.** were for (c) Let-7b•P<sub>7b</sub>,  $\tau_{off}=1.7\pm0.6$  s, and (d) Let-7c•P<sub>7b</sub>,  $\tau_{off}=11\pm3$  ms at +180 mV. Solutions contained 3 M/0.5 M cis/trans KCl and 10 mM Tris (pH7.2).

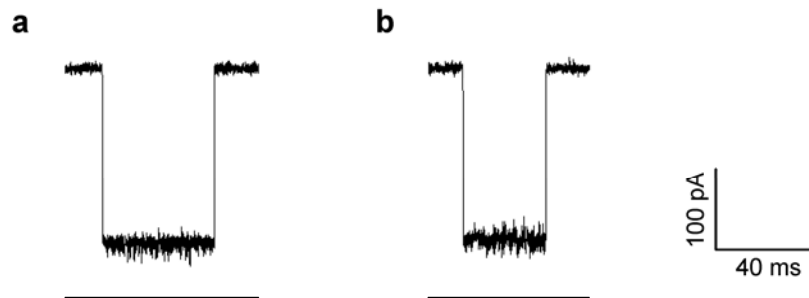


**Figure S5.** Typical current blocks produced by the Let-7b•P<sub>7b</sub> complex trapped in the K131D pore (**a**) and by the spontaneous gating of the K131D pore (**b**). The two types of blocks are distinguishable in the current pattern. The Let-7b•P<sub>7b</sub> signature is characterized by fast downward flicking, while the pore gating block does not feature it.

## **S1. Computational structure model of the microRNA•probe complex**

The sequences of miRNA Let-7b and its probe P<sub>7b</sub> are shown in Table S1. The Let-7b•P<sub>7b</sub> complex consists of three domains: the 11-amino acid peptide domain including 8 cationic residues, the 10-basepair miRNA•PNA duplex, and the 12-nucleotide single-stranded miRNA (ss-miRNA) domain. The conformation for each domain was built separately. The three domains were finally assembled into a Let-7b•P<sub>7b</sub> structure. The conformation of the miRNA•PNA duplex was created using an experimentally determined structure (PDB id: 176D) as the template. For the peptide and ss-miRNA domains, both oligomers are flexible and can adopt a large number of conformations. We used the CABS and PULCHRA models<sup>1-3</sup> to generate peptide conformations, and the Vfold model<sup>4</sup> to construct ss-miRNA conformations. The CABS model gives a reduced representation for protein conformations<sup>1,2</sup> and the PULCHRA model provides a computationally efficient method for constructing the all-atom protein structure from the backbone C $\alpha$  atoms<sup>3</sup>. Vfold is a free energy-based model for RNA 3D structure prediction<sup>4</sup>. The model has been successful in predicting a broad range of RNA structures and functions such as miRNA-target interactions<sup>5</sup>. The structure of the Let-7b•P<sub>7b</sub> complex was constructed as the assembly of the conformations of the three domains. Specifically, the C $\alpha$  atoms between the peptide C-terminal and the PNA N-terminal were joined, and the 5'-end phosphate of the miRNA•PNA duplex was linked with the 3'-end C4' atom of ss-miRNA. Using these models, we have randomly generated 20 peptide conformations and 100 ss-miRNA conformations, then constructed an ensemble of a total of 2000 conformations for the probe and ss-miRNA complex. By calculating the electrostatic free energies for different conformations, we computed the Let-7b•P<sub>7b</sub> complex structure that has the lowest electrostatic free energy (see Fig. 3a).



#### Reference List

1. Kolinski, A. Protein Modeling and Structure Prediction With a Reduced Representation. *Acta Biochim.Pol.* **2004**, 51, 349-371.
2. Kolinski, A.; Skolnick, J. Reduced Models of Proteins and Their Applications. *Polymer* **2004**, 45, 511-524.
3. Rotkiewicz, P.; Skolnick, J. Fast Procedure for Reconstruction of Full-Atom Protein Models From Reduced Representations. *J Comput.Chem* **2008**, 29, 1460-1465.
4. Cao, S.; Chen, S. J. Predicting RNA Folding Thermodynamics With a Reduced Chain Representation Model. *RNA* **2005**, 11, 1884-1897.
5. Cao, S.; Chen, S. J. Predicting Kissing Interactions in MicroRNA-Target Complex and Assessment of MicroRNA Activity. *Nucleic Acids Res* **2012**, 40, 4681-4690.